

Numerical Determination of Flow Corrective Inserts for Granular Materials in Conical Hoppers*

PIERRE-ALAIN GREMAUD[†], DAVID G. SCHAEFFER[‡], AND MICHAEL SHEARER[†]

Center for Research in Scientific Computation and
Department of Mathematics, North Carolina State University, Raleigh, NC 27695-8205.[†]
Department of Mathematics, Duke University, Durham, NC 27706.[‡]

The flow of granular materials in hoppers is studied. In industrial applications, inserts of various sizes and shapes are often used to improve the flow properties and get rid of undesirable effects such as material sticking to the walls, funnel flow, arching, etc. We study the case of inverted conical inserts in conical hoppers. In spite of the complexity of the phenomenon as observed in practice, existing methods assume in general a radial structure of the stress and velocity fields. A new numerical approach to the problem of designing “optimal” inserts is proposed and tested. It allows for non purely radial solutions. General comments about the overall approach and its relationship with experiments are offered.

1. Introduction. In the 1960’s, Jenike [2] proposed a special solution of steady state equations describing the flow of a cohesionless granular material in a conical hopper. This solution, the so-called *radial flow solution* is the basis for much work on the design of industrial hoppers for the handling of many different kinds of granular materials [3].

The radial solution predicts stresses and velocities in a *mass flow hopper*, in which the material flows smoothly everywhere. By contrast, *funnel flow* is irregular, with material flowing primarily, or entirely, down a central funnel, leaving a stagnant region adjacent to the hopper wall. In such circumstances, the radial solution does not predict the flow; moreover, the radial solution breaks down near the transition from mass flow to funnel flow.

The flow characteristics in a funnel flow hopper may be improved by installing rigid inserts within the hopper, to divert the flow out toward the stagnant zone. In this paper, we begin an analysis of conical inserts. We consider three dimensional axisymmetric flow in the space between a small inverted cone (the insert) and a large cone (the hopper) that have the same axis of rotation, as shown in Figure 1.1.

In 1964, Johanson [5] proposed a design procedure for conical inserts. The basis for the procedure is to regard the flow in a region between the insert and the hopper wall as being well approximated by a plane radial flow, neglecting the curvature of the insert and of the hopper wall. The intuition here is that the space between the hopper wall and the insert is nearly a wedge, with slightly curved walls, so that the curvature of the hopper and of the insert should represent a higher order correction to a plane radial solution. Of course, this notion becomes untenable near the vertex of the insert.

*This project was supported by the National Science Foundation through grant DMS 9803305. Moreover, the first author was supported by the Army Research Office through grants DAAH04-95-1-0419 and DAAH04-96-1-0097, and by the North Carolina Supercomputing Center. The second author was supported by the National Science Foundation through grant DMS 9504577. The third author was supported by National Science Foundation grant DMS 9504583, and by Army Research Office grant (DAAG55-98-10128).

In this paper, we explore Johanson's idea by introducing an asymptotic expansion of the solution about $r = 0$ in the coordinates of Figure 1.1. In the figure, we show toroidal coordinates (r, θ, ϕ) , in which ϕ is the angle of rotation about the axis, and r, θ are plane polar coordinates in the plane $\phi = \text{const}$, centered at the point at which the insert would intersect the hopper if the insert were continued as shown by the dashed line. The plane radial solution appears as the leading order term in the asymptotic expansion. We then formulate equations for the next order terms, representing a correction to the plane radial solution. The purpose of the correction is to partially alleviate some of the obvious shortcomings [10, p.327] of the purely radial approach of [5]. The equations (at both orders) are solved numerically for representative physical parameters.

While it would be reasonable to expect the asymptotic expansion to be valid near $r = 0$, the physical domain in fact involves values of r away from zero. In particular, near the vertex of the insert, r/a is of order one, so that the asymptotic expansion is suspect. This simple observation suggests that Johanson's design procedure is probably incorrect. However, we find that the first order correction is small for some ranges of parameters, specifically for fairly steep and fairly smooth walls. While this is not the most significant range, as funnel flow is expected for rough walls and less steep hoppers, it does suggest that the plane radial solution may be a coarse but useful approximation in some parameter range.

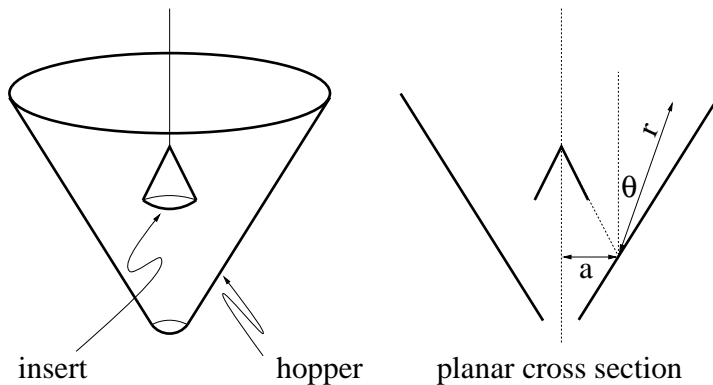


FIGURE 1.1. *Conical hopper with an inverted cone insert.*

Incidentally, the mass flow in a conical hopper is thought to be close to radial apart from thin transition layers near the top and the bottom of the hopper, even when the hopper is only a part of a more complex geometry, such as a cylindrical bin above the hopper, and a cylindrical feeder below. Correspondingly, it is plausible that a fully mobilized flow between the insert and the hopper wall should be largely independent of the flow above and below the insert.

The outline of the paper is as follows. In Section 2, we describe the equations of motion and constitutive laws. The asymptotic expansion is formulated in Section 3. In Section 4, we present numerical results for the first two terms in the expansion. Conclusions are offered in Section 5.

2. Equations of Motion. We consider steady incompressible flow in which the particles have no motion in the axial (or φ) direction. Then the dependent variables

reduce to four components of stress and two of velocity:

$$T = \begin{pmatrix} T_{rr} & T_{r\vartheta} & 0 \\ T_{r\vartheta} & T_{\vartheta\vartheta} & 0 \\ 0 & 0 & T_{\varphi\varphi} \end{pmatrix} \quad v = \begin{pmatrix} v_r \\ v_\vartheta \\ 0 \end{pmatrix}. \quad (2.1)$$

The equations of motion are

$$\nabla \cdot T = \rho g, \quad (2.2)$$

in which ρ is the density, taken to be constant, and the vector g is the acceleration due to gravity, and

$$\nabla \cdot v = 0, \quad (2.3)$$

Equations (2.2) represent the balance of forces in the material, while equation (2.3) expresses incompressibility. Note that because gravity has no component in the axial direction, T is independent of φ , and given the form (2.1) of the stress tensor T , equations (2.2) reduce to two equations, so that the system (2.2,2.3) consists of three equations in the six unknowns of (2.1).

Added to these equations are constitutive laws. Let $p = \text{tr } T/3$ be the *average stress*, more precisely the average of the principal stresses $\sigma_i, i = 1, 2, 3$, the eigenvalues of T . Assuming plastic deformation everywhere, we impose the *von Mises yield condition* [7]

$$\sum_{i=1}^3 (\sigma_i - p)^2 = 2 \sin^2 \delta p^2, \quad (2.4)$$

where δ is the angle of internal friction. Finally, we have the *flow rule*, which relates the stress to the deformation through the *strain rate tensor*, defined as

$$V = -\frac{1}{2}(\nabla v + \nabla v^T).$$

The condition of *alignment*, the flow rule used here, is that there exists a scalar $q > 0$ such that

$$V = q(T - pI). \quad (2.5)$$

In particular, since $\nabla \cdot v = -\text{tr } V$, and the right hand side of (2.5) has zero trace, the flow rule is consistent with the incompressibility condition (2.3). Equation (2.4) is a single algebraic constraint on the stress, while equation (2.5) reduces to two equations relating the stress and velocity gradients. Thus, equations (2.2–2.5) represent a set of six equations in the six unknowns of (2.1).

In the coordinates of Figure 1.1, the strain rate tensor becomes

$$V = \begin{pmatrix} -\partial_r v_r & (-\frac{1}{r}\partial_\vartheta v_r - \partial_r v_\vartheta + \frac{v_\vartheta}{r})/2 & 0 \\ (-\frac{1}{r}\partial_\vartheta v_r - \partial_r v_\vartheta + \frac{v_\vartheta}{r})/2 & -\frac{1}{r}(\partial_\vartheta v_\vartheta + v_r) & 0 \\ 0 & 0 & -\frac{v_r \sin \vartheta + v_\vartheta \cos \vartheta}{a + r \sin \vartheta} \end{pmatrix},$$

and the six equations are

$$\begin{aligned} \partial_r T_{rr} + \frac{1}{r} \partial_\vartheta T_{r\vartheta} + \left(\frac{1}{r} + \frac{\sin \vartheta}{a + r \sin \vartheta}\right) T_{rr} + \frac{\cos \vartheta}{a + r \sin \vartheta} T_{r\vartheta} \\ - \frac{1}{r} T_{\vartheta\vartheta} - \frac{\sin \vartheta}{a + r \sin \vartheta} T_{\varphi\varphi} = -\rho g \cos \vartheta, \end{aligned} \quad (2.6)$$

$$\partial_r T_{r\vartheta} + \frac{1}{r} \partial_\vartheta T_{\vartheta\vartheta} + \left(\frac{2}{r} + \frac{\sin \vartheta}{a + r \sin \vartheta} \right) T_{r\vartheta} + \frac{\cos \vartheta}{a + r \sin \vartheta} (T_{\vartheta\vartheta} - T_{\varphi\varphi}) = \rho g \sin \vartheta, \quad (2.7)$$

$$(T_{rr} - p)^2 + (T_{\vartheta\vartheta} - p)^2 + (T_{\varphi\varphi} - p)^2 + 2T_{r\vartheta}^2 = 2 \sin^2 \delta p^2, \quad (2.8)$$

$$\frac{\frac{\sin \vartheta}{a + r \sin \vartheta} v_r + \frac{\cos \vartheta}{a + r \sin \vartheta} v_\vartheta}{\frac{1}{r} \partial_\vartheta v_\vartheta + \frac{1}{r} v_r} = \frac{T_{\varphi\varphi} - p}{T_{\vartheta\vartheta} - p}, \quad (2.9)$$

$$\frac{1}{2} \frac{\partial_r v_\vartheta + \frac{1}{r} \partial_\vartheta v_r - \frac{1}{r} v_\vartheta}{\frac{1}{r} \partial_\vartheta v_\vartheta + \frac{1}{r} v_r} = \frac{T_{r\vartheta}}{T_{\vartheta\vartheta} - p}, \quad (2.10)$$

$$\partial_r v_r + \frac{1}{r} \partial_\vartheta v_\vartheta + \left(\frac{1}{r} + \frac{\sin \vartheta}{a + r \sin \vartheta} \right) v_r + \frac{\cos \vartheta}{a + r \sin \vartheta} v_\vartheta = 0. \quad (2.11)$$

Equations (2.6) and (2.7) are the stress equilibrium conditions, while (2.8) is the von Mises yield condition. Equations (2.9) and (2.10) are direct consequences of the flow rule (2.5). Finally, (2.11) is the continuity equation expressing incompressibility.

Additionally, we impose the following boundary conditions at the insert ($\vartheta = \vartheta_1$) and at the hopper wall ($\vartheta = \vartheta_2$):

$$T_{r\vartheta}(\vartheta_1) = \mu T_{\vartheta\vartheta}(\vartheta_1) \quad T_{r\vartheta}(\vartheta_2) = -\mu T_{\vartheta\vartheta}(\vartheta_2), \quad (2.12)$$

$$v_\vartheta(\vartheta_1) = 0 \quad v_\vartheta(\vartheta_2) = 0. \quad (2.13)$$

Equation (2.12) expresses the law of sliding friction. For simplicity, we assume the same coefficient of wall friction μ for both insert and hopper.

3. Expansion for the hopper/insert system. In the case of the hopper/insert problem, there is no similarity solution. For $a \neq 0$, $a \gg r$, see Figure 1.1, we consider instead the following expansion

$$\begin{aligned} T &= rT^0(\vartheta) + r^2T^1(\vartheta) + \dots, \\ v &= \frac{1}{r}v^0(\vartheta) + v^1(\vartheta) + \dots \end{aligned} \quad (3.1)$$

We introduce new Sokolovskii variables to rewrite the first three components of the stress tensor. For $k = 0, 1$, we set

$$\begin{pmatrix} T_{rr}^k(\vartheta) & T_{r\vartheta}^k(\vartheta) \\ T_{r\vartheta}^k(\vartheta) & T_{\vartheta\vartheta}^k(\vartheta) \end{pmatrix} = \sigma^k(\vartheta) \mathbb{I} + \tau^k(\vartheta) \begin{pmatrix} -\cos 2\psi^k(\vartheta) & -\sin 2\psi^k(\vartheta) \\ -\sin 2\psi^k(\vartheta) & \cos 2\psi^k(\vartheta) \end{pmatrix}. \quad (3.2)$$

Relations (3.1) and (3.2) are then substituted in (2.6–2.11), and the coefficients of equal power of r equated. Only terms of order 0 and 1 are considered here.

From (2.9), one observes

$$T_{\varphi\varphi}^0 = p^0 = \sigma^0. \quad (3.3)$$

Using (2.8), it then follows that

$$\tau^0 = \sigma^0 \sin \delta \quad (3.4)$$

Using relations (2.6) and (2.7) lead to the system

$$\begin{pmatrix} -\sin \delta \sin 2\psi^0 & -2\sigma^0 \sin \delta \cos 2\psi^0 \\ 1 + \sin \delta \cos 2\psi^0 & -2\sigma^0 \sin \delta \sin 2\psi^0 \end{pmatrix} \begin{pmatrix} \sigma^0 \\ \psi^0 \end{pmatrix}' + \begin{pmatrix} \sigma^0(1 - 3 \sin \delta \cos 2\psi^0) \\ -3\sigma^0 \sin \delta \sin 2\psi^0 \end{pmatrix} = \begin{pmatrix} -\rho g \cos \vartheta \\ \rho g \sin \vartheta \end{pmatrix}, \quad \vartheta \in (\vartheta_1, \vartheta_2). \quad (3.5)$$

System (3.5) for σ^0 and ψ^0 is completed by imposing two boundary conditions

$$T_{r\vartheta}(\vartheta_1) = \mu T_{\vartheta\vartheta}(\vartheta_1) \quad T_{r\vartheta}(\vartheta_2) = -\mu T_{\vartheta\vartheta}(\vartheta_2).$$

These equations yield boundary conditions on ψ^0 , using (3.2) with $k = 0$, and (3.4):

$$\psi^0(\vartheta_1) = -\psi_w \quad \psi^0(\vartheta_2) = \psi_w, \quad (3.6)$$

with $\psi_w = \frac{\arctan \mu}{2} + \frac{1}{2} \arcsin \left(\frac{\sin(\arctan \mu)}{\sin \delta} \right) = \frac{1}{2} \left(\Phi + \arcsin \left(\frac{\sin \Phi}{\sin \delta} \right) \right)$ where Φ (given by $\mu = \tan \Phi$), is the angle of wall friction. Incidentally, the above relation makes sense only if the angle of wall friction Φ is no larger than the angle of internal friction δ , i.e., $\Phi \leq \delta$, or equivalently, $\mu \leq \tan \delta$. In practice, the roughness of the walls is usually such that this condition is comfortably satisfied [7, p.46]. The relationship between ψ_w and (μ, δ) is illustrated in Figure 3.1.

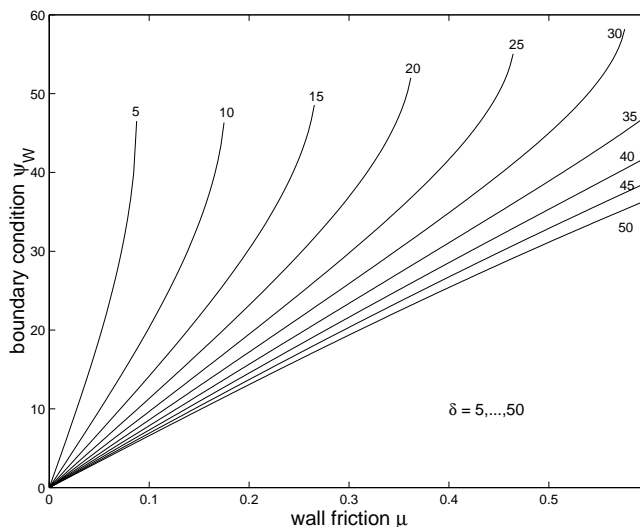


FIGURE 3.1. Dependence of the boundary condition ψ_w with respect to the wall friction μ for various values the angle of internal friction δ .

We remark that the above problem (3.5, 3.6), corresponding to the lowest order terms in expansion (3.1), is the same as the system governing stresses in Jenike's planar radial solution [7].

We now turn to the derivation of the equations for the first order terms. Using (2.9), we get

$$T_{\varphi\varphi}^1 = p^1 + \frac{\sin \vartheta}{a} \sigma^0 \sin \delta \cos 2\psi^0,$$

and thus, by definition of p^1

$$p^1 = \sigma^1 + \frac{\sin \vartheta}{2a} \sigma^0 \sin \delta \cos 2\psi^0. \quad (3.7)$$

This last relation is the first order analog to (3.3). Then (2.8) leads to

$$\tau^0 \tau^1 \cos 2(\psi^0 - \psi^1) = \sin^2 \delta \sigma^0 p^1,$$

and thus, by (3.4) and (3.7)

$$\tau^1 \cos 2(\psi^0 - \psi^1) = \sin \delta \left(\sigma^1 + \frac{\sin \vartheta}{2a} \sigma^0 \sin \delta \cos 2\psi^0 \right). \quad (3.8)$$

Equation (3.8) will be regarded as an equation for σ^1 , once ψ^1 and τ^1 have been determined. Equations for ψ^1 and τ^1 are obtained from (2.6) and (2.7), which yield

$$\begin{aligned} (-\tau^1 \sin 2\psi^1)' + 2\sigma^1 - 4\tau^1 \cos 2\psi^1 &= \frac{\sigma^0}{a} \sin \delta \sin(\vartheta + 2\psi^0), \\ (\sigma^1 + \tau^1 \cos 2\psi^1)' - 4\tau^1 \sin 2\psi^1 &= -\frac{\sigma^0}{a} \sin \delta \cos(\vartheta + 2\psi^0). \end{aligned} \quad (3.9)$$

From the form of these equations, we see that it is convenient to use new variables w, z for the stress components

$$w = \tau^1 \cos 2\psi^1, z = \tau^1 \sin 2\psi^1,$$

The first order counterpart to the boundary conditions (3.16) is found to be

$$\begin{aligned} -z(\vartheta_1) &= \mu(u(\vartheta_1) + w(\vartheta_1)), \\ z(\vartheta_2) &= \mu(u(\vartheta_2) + w(\vartheta_2)), \end{aligned}$$

where u is defined by

$$u = \frac{1}{\sin \delta} \left(w \cos 2\psi^0 + z \sin 2\psi^0 - \frac{\sin^2 \delta}{2a} \sigma^0 \sin \vartheta \cos 2\psi^0 \right). \quad (3.10)$$

We now turn to the determination of the velocity equations, at the zeroth and first orders. At the zero-th order, equation (2.11) reduces to

$$\partial_\vartheta v_\vartheta^0 = 0,$$

and thus, since v_ϑ has to vanish on the boundary, we have

$$v_\vartheta^0 \equiv 0. \quad (3.11)$$

The equation for v_r^0 is obtained from (2.10), which becomes

$$\partial_\vartheta v_r^0 = -2 v_r^0 \tan 2\psi^0. \quad (3.12)$$

This equation is homogeneous in v_r^0 , so it determines v_r^0 apart from a constant multiple. This multiple could be fixed by imposing the withdrawal rate $\rho \int v_r r d\vartheta$. In computations, we set $v_r^0(0) = 1$. As for the stress field at lowest order, the velocity field given by (3.11), (3.12) is the same as for Jenike's plane radial solution [7].

To obtain the first order equations for the velocities, we first note

$$\frac{T_{r\vartheta}}{T_{\vartheta\vartheta} - p} = \frac{T_{r\vartheta}^0}{T_{\vartheta\vartheta}^0 - p^0} + r \left(\frac{T_{r\vartheta}^1}{T_{\vartheta\vartheta}^0 - p^0} - \frac{T_{r\vartheta}^0 (T_{\vartheta\vartheta}^1 - p^1)}{(T_{\vartheta\vartheta}^0 - p^0)^2} \right) + \dots$$

Equation (2.10) then leads to

$$\partial_{\vartheta} v_r^1 + 2 \tan 2\psi^0 (\partial_{\vartheta} v_{\vartheta}^1 + v_r^1) - v_{\vartheta}^1 = -\frac{\sin 2\psi^0}{\sigma^0 \sin \delta \cos^2 2\psi^0} \left(2w + \frac{\sin \vartheta}{a} \sigma^0 \sin \delta \cos 2\psi^0 \right) v_r^0. \quad (3.13)$$

On the other hand, (2.11) yields the equation for v_{ϑ}^1 , which is found to be

$$\partial_{\vartheta} v_{\vartheta}^1 + v_r^1 = -\frac{\sin \vartheta}{a} v_r^0. \quad (3.14)$$

The fact that v_{ϑ} vanishes on the boundary provides the additional conditions necessary to close our system

$$v_{\vartheta}^1(\vartheta_1) = v_{\vartheta}^1(\vartheta_2) = 0.$$

For convenience, the equations are rewritten in a more compact form.

$$\begin{pmatrix} A & B & 0 & 0 & 0 & 0 & 0 \\ C & D & 0 & 0 & 0 & 0 & 0 \\ 0 & 0 & 0 & E & 0 & 0 & 0 \\ F & G & H & I & 0 & 0 & 0 \\ 0 & 0 & 0 & 0 & 1 & 0 & 0 \\ 0 & 0 & 0 & 0 & 0 & 1 & J \\ 0 & 0 & 0 & 0 & 0 & 0 & 1 \end{pmatrix} \begin{pmatrix} \sigma^0 \\ \psi^0 \\ w \\ z \\ v_r^0 \\ v_r^1 \\ v_{\vartheta}^1 \end{pmatrix}' + \begin{pmatrix} K \\ L \\ M \\ N \\ O \\ P \\ Q \end{pmatrix} = \begin{pmatrix} -\rho g \cos \vartheta \\ \rho g \sin \vartheta \\ 0 \\ 0 \\ 0 \\ 0 \\ 0 \end{pmatrix}. \quad (3.15)$$

The above system of ODEs is closed with the following boundary conditions, deriving from (2.12, 2.13)

$$\psi^0(\vartheta_1) = -\psi_w \quad \psi^0(\vartheta_2) = \psi_w, \quad (3.16)$$

$$-z(\vartheta_1) = \mu(\sigma^1(\vartheta_1) + w(\vartheta_1)), \quad z(\vartheta_2) = \mu(\sigma^1(\vartheta_2) + w(\vartheta_2)), \quad (3.17)$$

$$v_{\vartheta}^1(\vartheta_1) = 0 \quad v_{\vartheta}^1(\vartheta_2) = 0, \quad (3.18)$$

where the various quantities $A, B, C, \text{etc.}$ appearing in (3.15) are described in the Appendix. Note that there are no boundary conditions on σ^0 , w and v_r^1 . Further, (3.15) is well posed if we add one condition on v_r^0 , such as $v_r^0(0) = 1$.

By examining the structure of the above system, one can see that upon approximation by the series (3.1), the stress equations can be solved both at the zero-th and the first order, independently of the velocity equations (this is not true of the PDE's). We can thus decompose the ODE into three problems of increasing complexity by solving a problem for the zero-th order stress terms first, then by solving for the first order stress terms, and finally by solution for the components of the velocity. With the notation of (3.15), the three corresponding matrices are respectively

$$M_0 = \begin{pmatrix} A & B \\ C & D \end{pmatrix}, \quad M_1 = \begin{pmatrix} A & B & 0 & 0 \\ C & D & 0 & 0 \\ 0 & 0 & 0 & E \\ F & G & H & I \end{pmatrix}, \quad M = \begin{pmatrix} A & B & 0 & 0 & 0 & 0 & 0 \\ C & D & 0 & 0 & 0 & 0 & 0 \\ 0 & 0 & 0 & E & 0 & 0 & 0 \\ F & G & H & I & 0 & 0 & 0 \\ 0 & 0 & 0 & 0 & 1 & 0 & 0 \\ 0 & 0 & 0 & 0 & 0 & 1 & J \\ 0 & 0 & 0 & 0 & 0 & 0 & 1 \end{pmatrix}. \quad (3.19)$$

Again, we stress that only the zero-th order stress terms appear in the equation corresponding to M_0 . Likewise, the M_1 -equation only contains zero and first order stress terms. This fact is used in the next section. Further, we observe that each of the

three systems M_0 , M_1 and M is singular under the same condition. Indeed, one easily checks

$$\begin{aligned}\det M_0 &= 2\sigma^0 \sin \delta (\cos 2\psi^0 + \sin \delta), \\ \det M_1 = \det M &= -2\sigma^0 \sin^2 \delta (\cos 2\psi^0 + \sin \delta)^2.\end{aligned}$$

Therefore, putting aside the particular case $\sigma^0 = 0$ and/or $\sin \delta = 0$, the stress equations are singular if

$$\cos 2\psi^0 + \sin \delta = 0. \quad (3.20)$$

The system of three velocity equations (3.12–3.14) is singular whenever

$$\psi^0 = \pi/4 = 45^\circ. \quad (3.21)$$

We will use this condition to numerically determine the stagnant part of the flow in the next section.

4. Numerical results. The numerical method is based on the two following main steps

(1) use of a Runge-Kutta-Fehlberg 4(5) method with automatic step size selection for integrating the ODEs (i.e., a 4th order Runge-Kutta where the local truncation error is estimated through a fifth order formula, and is then used for step size selection);

(2) use of an inexact Newton method for solving the nonlinear problems arising from the shooting steps (see below).

As described in the previous section, we have to solve a boundary value problem consisting of seven nonlinear coupled ODEs. Numerically, this is done by solving a sequence of initial value problems where the “missing” initial values are sought so as to satisfy the prescribed boundary conditions, i.e., the so-called shooting method is used.

As is well known, the shooting method can lead to various problems in practice. As an alternative to multiple shooting, the shooting process is done here in several steps, in order to take advantage of the block structure of the system (3.15). The approach is simpler than multiple shooting and works well in the present context.

First, the equation corresponding to M_0 , (3.19.1), is solved for the 0th order stress terms σ^0 and ψ^0 , is solved. The boundary conditions (3.16) are adjusted through shooting on σ . Second, the system corresponding to M_1 , (3.19.2), is solved. The boundary conditions (3.17) are adjusted through shooting on w . Finally, the system with M , (3.19.3) is solved, and the boundary conditions (3.18) are adjusted through shooting on v_r^1 . We omit the details.

4.1 General properties of the flow. Typical solutions are illustrated below. Note that the parameters a , ρ and g are all set equal to 1 throughout. Tolerance parameters have been set equal to 10^{-10} for both the ODEs and the nonlinear solvers.

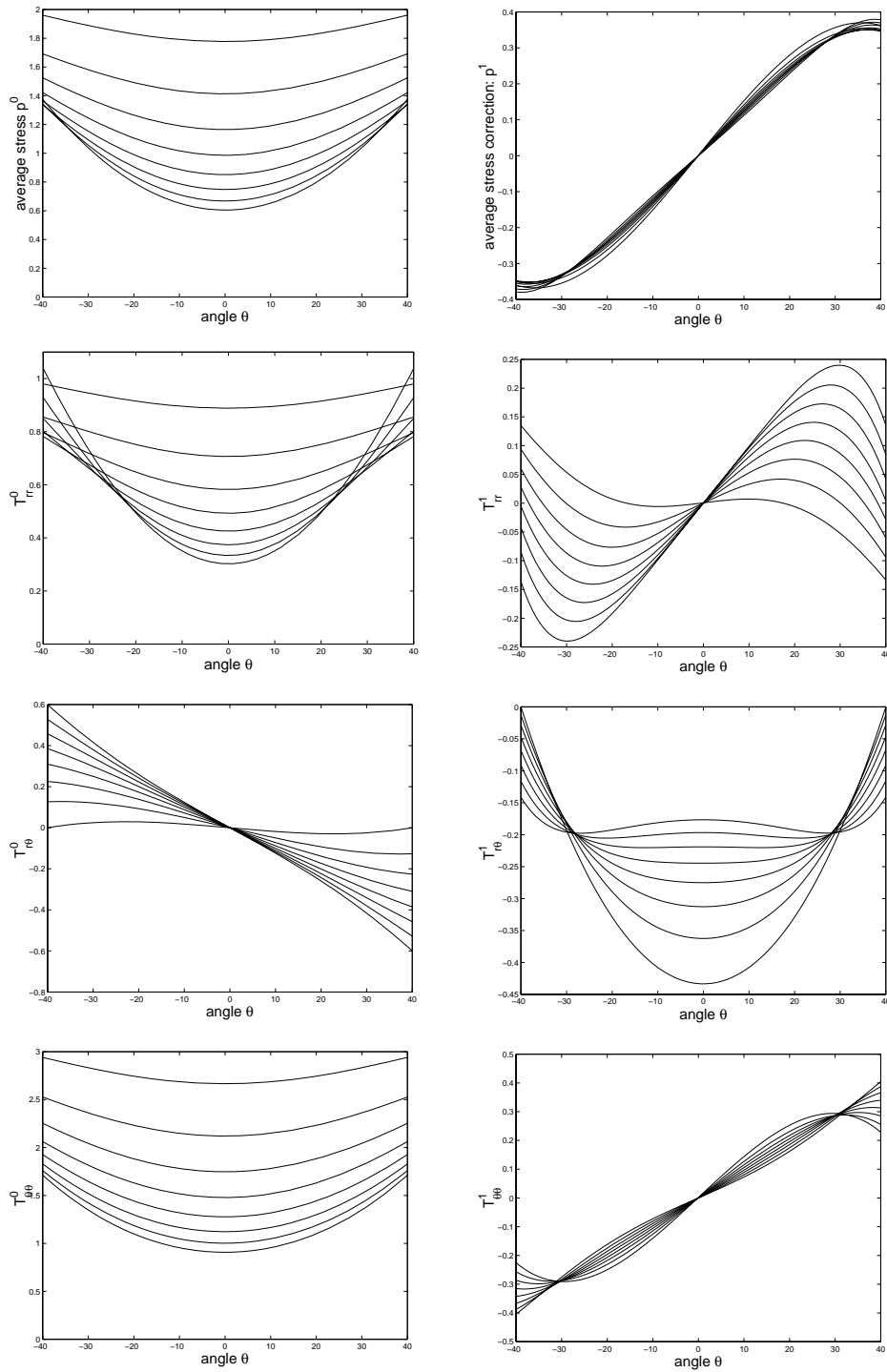


FIGURE 4.1. Stress components of the problem with conical insert: angle of friction $\delta = 30^\circ$, half opening angle = 40° and wall friction $\mu = i/20$, $i = 0, \dots, 7$. In all the pictures except $T^1_{r\theta}$, $\mu = 0$ corresponds to the flatter curve. Left column: zeroth order terms, right column: first order terms.

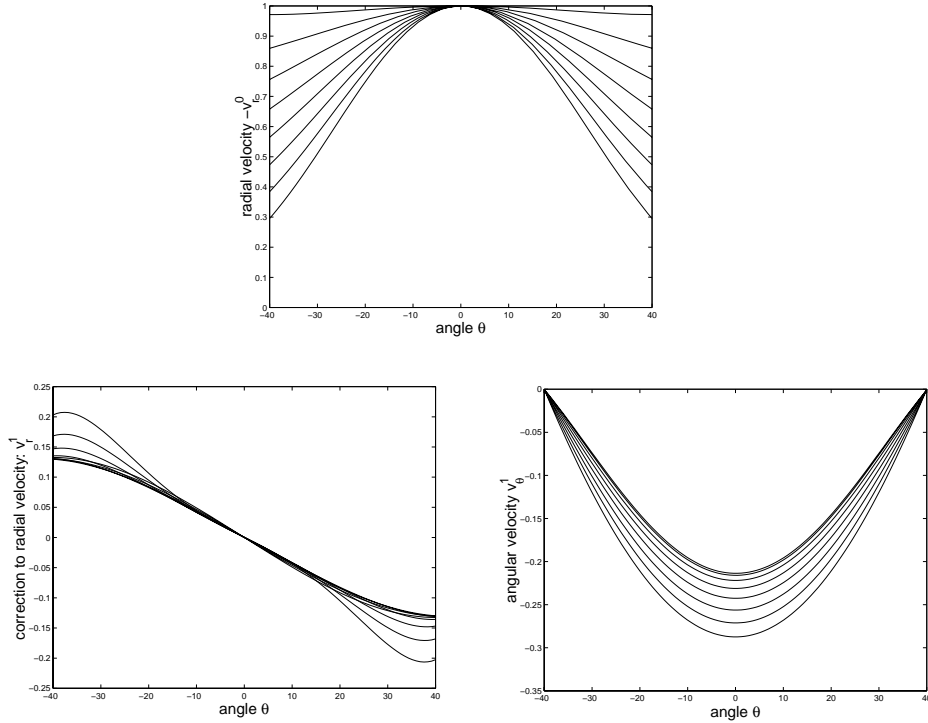


FIGURE 4.2. Velocity components of the problem with conical insert: angle of friction $\delta = 30^\circ$, half opening angle = 40° and wall friction $\mu = i/20, i = 0, \dots, 7$. In the first two pictures pictures, $\mu = 0$ corresponds to the flatter curve; the order is reversed for v_θ^1 .

Note that the above velocity fields have been normalized by setting $v_r^0(0) = 1$. The departure from a purely radial structure is visible by inspection of Figure 4.1 and 4.2. The flow is also illustrated in Figure 4.3 by plotting streamlines of the velocity field including zero-th and first order terms.

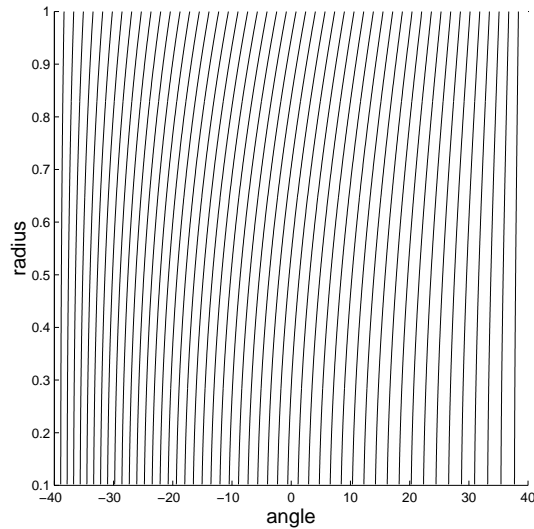


FIGURE 4.3. Streamlines from the velocity field.

4.2 Determination of the stagnant part of the flow. As noted at the end of Section 3, the stress equations become singular when

$$\psi_0 = \frac{\arccos(-\sin \delta)}{2} > \frac{\pi}{4}, \quad (4.1)$$

whereas the velocity equations become singular when

$$\psi_0 = \frac{\pi}{4}, \quad (4.2)$$

I.e., the velocity equations become singular “before” the stress equations. In other words, we can solve the M_0 -system, corresponding to the zero-th order stress terms and determine where the 0-th order velocity equation becomes singular. Following [7], we *interpret* the part of the flow beyond the point where the velocity field becomes singular as corresponding to the *stagnant* portion of the flow. This way, a “partial map” of the failure mode of the insert strategy is obtained. The present analysis implicitly assumes the stagnant zone to be radial, which is rarely the case in practice. The position of the critical ray, if it exists, separating the moving and stagnant parts of the flow is measured in the coordinate system of Figure 1.1 by a critical angle ϑ^* .

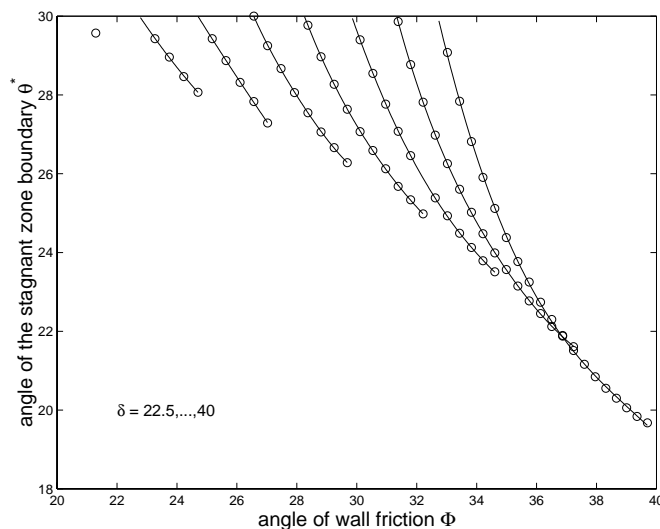


FIGURE 4.4. Dependence of the stagnant zone boundary angle with angle of wall friction in a hopper with a 30° half angle for various values of the internal angle of friction δ between 22.5° (left) and 40° (right).

In Figure 4.4, the critical angle ϑ^* is plotted as a function the angle of wall friction, $\Phi = \arctan(\mu)$ for a hopper with a 30° half opening angle, for various values of the angle of internal friction δ . The algorithm consists of computing stresses with hopper and insert angles set to $\vartheta = 30^\circ$, for various values of Φ , and fixed δ in the range $22.5^\circ \leq \delta \leq 40^\circ$. For small Φ , $\psi^o(\vartheta), \pi/4$ everywhere, but as Φ increases, there is an angle ϑ^* at which (4.2) is satisfied. This marks the stagnant zone, and is plotted in Figure 4.4. As Φ is increased further, the stresses can still be plotted, until ψ^o first satisfies (4.1) at some value of ϑ , at which point the stress equations break down, and the calculation terminates, corresponding to the end of the corresponding curve in Figure 4.4.

A value of $\vartheta^* = 30^\circ$ corresponds to no stagnant zone. For values of $\delta < 20^\circ$, no stagnant zone was predicted. One observes that for each considered value of the internal angle of friction δ , there is a critical value of the wall friction, below which there is no stagnant region, and above which a stagnant appears. This critical value increases with δ . Further, for a fixed δ , the width of the stagnant part of the flow increases with the wall friction until the stress equations break down at the end of the curve, where (4.1) at some value of ϑ .

5. Conclusions. The flow of granular materials in conical hoppers with flow correcting inserts is considered. It is shown that the usual assumption used in practice of a radial structure of the flow is questionable. The analysis is based on an expansion in powers of the radius r of the physical variables (stress, velocity). For each variable, the first two lowest order terms are kept. They correspond respectively to the standard approach of Jenike [2] and to new correcting terms proposed here. For most values of the parameters, the corrections are numerically found to be non negligible (size up to the order of that of the lowest order terms!). This shows that not only should the radial solution be used with caution in the present context, but that even terms including first order corrections might not accurately capture the behavior of the true solution, due to possibly large higher order terms. The addition of higher still order terms to the present approach is awkward at best. Future work will concentrate on the resolution of the full system of partial differential equations (2.6–2.11) [1].

Acknowledgments. The authors are grateful to David Craig, John Carson, Hermann Purutyan and Tony Royal at Jenike & Johanson, Inc., for several stimulating discussions.

REFERENCES

- [1] P. A. GREMAUD, J. V. MATTHEWS, Numerical simulation of granular flows in hoppers, In preparation.
- [2] A. JENIKE, Gravity flow of bulk solids, *Bulletin No. 108, Utah Eng. Expt. Station, University of Utah, Salt Lake City.*
- [3] T. A. ROYAL, Private Communication, Jenike & Johanson, Inc.
- [4] J. R. JOHANSON, Stress and velocity fields in the gravity flow of bulk solids, *J. Appl. Mech.*, 31 (1964), pp. 499–506.
- [5] J. R. JOHANSON, The use of flow-corrective inserts in bins, *Transactions of the ASME* (1966), pp. 224–230.
- [6] S.B.M. MOREEA AND R.M. NEDDERMAN, Exact Stress and Velocity Distributions in a Cohesionless Material Discharging from a Conical Hopper, *Chem. Eng. Sc.*, 51 (1996), pp. 3931–3942.
- [7] R.M. NEDDERMAN, *Statics and Kinematics of Granular Materials*, Cambridge University Press, 1992.
- [8] E. B. PITMAN, The stability of granular flow in converging hoppers, *SIAM J. Appl. Math.*, 48 (1988), pp. 1033–1052.
- [9] D. G. SCHAEFFER, Instability in the evolution equations describing incompressible granular flow, *J. Diff. Eqs.*, 66 (1987), pp. 19–50.
- [10] U. TÜZÜN AND R. M. NEDDERMAN, Gravity flow of granular materials round obstacles—I: investigation of the effects of inserts on flow patterns inside a silo, *Chem. Eng. Sc.*, 40 (1985), pp. 325–336.

Appendix. The coefficients of the system (3.15) are as follows

$$\begin{aligned} A &= -\sin \delta \sin 2\psi^0, \\ B &= -2\sigma^0 \sin \delta \cos 2\psi^0, \end{aligned}$$

$$\begin{aligned}
C &= 1 + \sin \delta \cos 2\psi^0, \\
D &= -2\sigma^0 \sin \delta \sin 2\psi^0, \\
E &= \sin \delta, \\
F &= -\frac{\sin^2 \delta}{2a} \sin \vartheta \cos 2\psi^0, \\
G &= -2u \sin 2\psi^0 + 2v \cos 2\psi^0 + \frac{\sin^2 \delta}{a} \sigma^0 \sin \vartheta \sin 2\psi^0, \\
H &= \cos 2\psi^0 + \sin \delta, \\
I &= \sin 2\psi^0, \\
J &= 2 \tan 2\psi^0, \\
K &= \sigma^0 (1 - 3 \sin \delta \cos 2\psi^0), \\
L &= -3\sigma^0 \sin \delta \sin 2\psi^0, \\
M &= u(4 \sin \delta - 2 \cos 2\psi^0) - 2v \sin 2\psi^0 + \frac{\sigma^0}{a} \sin^2 \delta \sin(\vartheta + 2\psi^0) + \sin \vartheta \cos 2\psi^0, \\
N &= -\frac{\sin^2 \delta}{2a} \sigma^0 \cos \vartheta \cos 2\psi^0 - 4v \sin \delta + \frac{\sigma^0}{a} \sin^2 \delta \cos(\vartheta + 2\psi^0), \\
O &= 2 \tan 2\psi^0 v_r^0, \\
P &= 2 \tan 2\psi^0 v_r^1 - v_\vartheta^1 + \frac{\sin 2\psi^0}{\sigma^0 \sin \delta \cos^2 2\psi^0} \left(2u + \frac{\sin \vartheta}{a} \sigma^0 \sin \delta \cos 2\psi^0 \right) v_r^0, \\
Q &= v_r^1 + \frac{\sin \vartheta}{a} v_r^0.
\end{aligned}$$

The relations between the variables of (3.15) of the physical components of the stress are follows

$$\begin{aligned}
T_{rr}^0 &= \sigma^0 (1 - \sin \delta \cos 2\psi^0), & T_{rr}^1 &= \sigma^1 - u, \\
T_{r\vartheta}^0 &= -\sigma^0 \sin \delta \sin 2\psi^0, & T_{r\vartheta}^1 &= -v, \\
T_{\vartheta\vartheta}^0 &= \sigma^0 (1 + \sin \delta \cos 2\psi^0), & T_{\vartheta\vartheta}^1 &= \sigma^1 + u, \\
T_{\varphi\varphi}^0 &= \sigma^0, & T_{\varphi\varphi}^1 &= \sigma^1 + \frac{\sin \vartheta}{3a} \sigma^0 \sin \delta \cos 2\psi^0,
\end{aligned}$$

$$\text{where } \sigma^1 = \frac{1}{\sin \delta} \left(u \cos 2\psi^0 + v \sin 2\psi^0 - \frac{\sin^2 \delta}{2a} \sigma^0 \sin \vartheta \cos 2\psi^0 \right).$$